Tetrahedron 64 (2008) 5410–5415

Contents lists available at ScienceDirect

Tetrahedron

journal homepage: www.elsevier.com/locate/tet

Synthesis of substituted dipyrido[3,2-*a*:2′,3′-*c*]phenazines and a new heterocyclic dipyrido[3,2-*f*:2′,3′-*h*]quinoxalino[2,3-*b*]quinoxaline

Fabio da Silva Miranda *, Aline Maria Signori, Juliano Vicente, Bernardo de Souza, Jacks Patrick Priebe, Bruno Szpoganicz, Norberto Sanches Gonçalves, Ademir Neves *

Departamento de Química, Universidade Federal de Santa Catarina, CP-476, 88040-900 Florianópolis, SC, Brazil

ARTICLE INFO

Article history:
Received 5 January 2008
Received in revised form 26 February 2008
Accepted 28 February 2008
Available online 4 March 2008

Keywords:
1,10-Phenanthroline-5,6-dione
dppz
dpq
Tetraazanaphthacene
B3LYP

ABSTRACT

Three new α,α′-diimine ligands were synthesized based on condensation of 1,10-phenanthroline-5,6-dione with 1,2-phenylenediamine derivatives using different approaches. All compounds were fully characterized by IR, ^{1}H and ^{13}C NMR, UV–visible, and MS spectroscopies. We report the first example of a dipyrido[3,2-*f*:2′,3′-*h*]quinoxalino[2,3-*b*]quinoxaline, which exhibits a strong absorption at 430 nm and an interesting electrochemical behavior. These new molecules may have biological potential and are of synthetic and technological importance.

1. Introduction

Ligands based on 1,10-phenanthroline (phen) and 2,2′-bipyridine (bpy) have been reported as potential prototypes in many applications including optical devices,[1,2] DNA intercalating,[3,4] with prospects regarding new drugs[5] and catalysts,[6] and supramolecular chemistry.[7,8] All these uses are based on the photo-physical and electrochemical properties of ligands and their metal complexes.[9] Molecules like dipyrido[3,2-*a*:2′,3′-*c*]phenazine (dppz)[10] and dipyrido[3,2-*f*:2′,3′-*h*]quinoxaline (dpq)[11] derivatives combine interesting properties, such as bidentate coordination ability, rigidity, and planar highly conjugated aromatic structure. Their π-accepting character and nitrogen sites enable them to be intercalated into DNA or promote H-bonds at the phenazine and quinoxaline moieties of these compounds, from the bpy moiety. In the photochemistry of ruthenium(II) and osmium(II) complexes with this class of ligands an electron excited at the metal center is transferred rapidly to the phenazine, resulting in an efficient charge separation useful for solar cells and other applications.

In connection with our interest in the search for new DNA cleaving agents[12,13] we present here the synthesis and complete characterization of a new polycyclic conjugate derivative from 1,10-phenanthroline-5,6-dione (**1**). Indeed, there are many publications in the literature on molecules that combine the phenanthroline or bipyridine moieties with the phenazine and quinoxaline units, but none with the tetraazanaphthacene moiety. This is the first example of a dipyrido[3,2-*f*:2′,3′-*h*]quinoxalino[2,3-*b*]quinoxaline ring (dpq-QX), which is a molecule containing the tetraazanaphthacene and bipyridine moieties together.

This new heterocyclic compound contains six condensation rings and six nitrogen atoms, two being coordinate donors at the phenanthroline moiety and four nitrogens from the tetraaza portion. This site is π-accepting and is able to coordinate metal centers and is also suited for H-bonding with H-donors like DNA-bases. In addition, this new heterocyclic compound also shows interesting optical and electrochemical properties. Tetraazanaphthacene has been described as an important heterocyclic compound in different areas, such as bridging mixed-valence metal complexes[14] and organic superconductors[15] and its photo-emission properties have been recently reported.[16] In this paper the synthesis of two new asymmetric dppz ligands with 2,1,3-thiadiazole (dppz–BTDZ) and sulfonic acid groups (dppz–SO_3) are also described, both with interesting optical and electrochemical behavior, and they may also provide new prototypes for DNA interaction.

The synthetic route to produce the three new compounds was based on the condensation of 1,10-phenanthroline-5,6-dione **1** with aromatic 1,2-diamines synthesized in many steps using three different approaches. All of them were based on the *o*-phenylenediamine **2** and obtained through adaptations from the literature

* Corresponding authors. Tel.: +55 48 3721 9852; fax: +55 48 3721 6850.
E-mail addresses: miranda@qmc.ufsc.br (F. da Silva Miranda), ademir@qmc.ufsc.br (A. Neves).

0040-4020/$ – see front matter © 2008 Elsevier Ltd. All rights reserved.
doi:10.1016/j.tet.2008.02.097

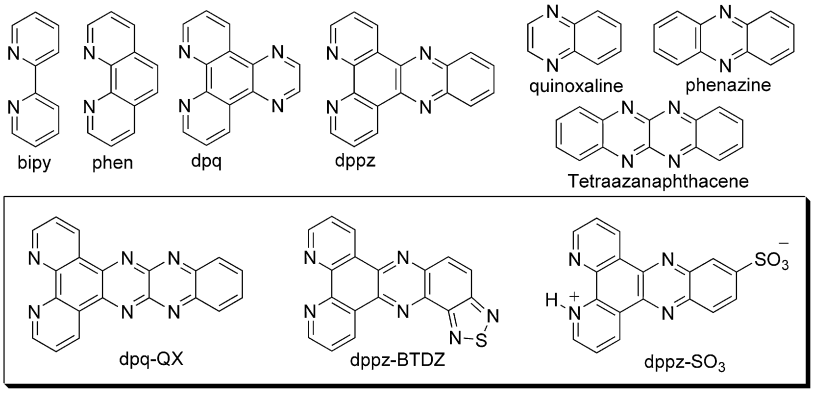

methods.[17–20] The *o*-phenylenediamine **2** has the advantage of reacting at different positions on the benzene ring or amino groups. We explored this feature to produce the symmetric 2,3-diaminequinoxaline **5** through the three-step procedure[17] as described by Carmack and shown in Scheme 1. Firstly, **2** was transformed into 2,3-dihydroxyquinoxaline **3** followed by reaction with thionyl chloride and DMF as the catalyst resulting in 2,3-dichloroquinoxaline **4** and amination with liquid ammonia in 80% yield.

The second amine was the 4,5-diamino-2,1,3-benzothiazole **9** obtained in four steps from **2**. The diamine was transformed into 2,1,3-benzothiadiazole **6**, as described by Dupont et al. using thionyl chloride in dichloromethane.[18] Nitration of **6** in a mixture of nitric and sulfuric acids at 10 °C gave 4-nitro-2,1,3-benzothiadiazole **7** in 80% yield as described in the literature.[19] The direct amination of **7** with hydroxylamine in methanolic potassium hydroxide gave 5-amino-4-nitro-2,1,3-benzothiazole **8**, which was reduced to 4,5-diamine-2,1,3-benzothiazole **9** with sodium dithionite in water.[20]

The sulfonation of phenylenediamine was performed via a new route using only concentrated sulfuric acid at 137 °C for 1 day. Cold water was then added resulting in a white precipitate, that was recrystallized in water affording the pure 3,4-diaminobenzenesulfonic acid **10** in 77% yield. The literature methods reported for the synthesis of 3,4-diaminobenzenesulfonic acid are more harsh, for example, sulfonation of *o*-phenylenediamine with H_2SO_4/SO_3,[21] SO_3,[22] or by reduction of 3-nitro-4-aminobenzenesulfonate with $HCl/SnCl_2$.[23] Our method offers a more simple approach to sulfonate **2**.

The dione **1** was prepared according to the literature[24] using $HNO_3/H_2SO_4/KBr$ to oxidize the 1,10-phenanthroline to 1,10-phenanthroline-5,6-dione **1** in high yields, which was then reacted with the diamines **5**, **9**, and **10** to form the new molecules **11**, **12**, and **13** in good yields. The reaction of the diamine **5** with **1** resulted in the new heterocyclic **11**, which shows a decreased solubility in most solvents in relation to dppz, probably due to π-stacking interactions and other intermolecular forces. Its structure has two conjugate pyrazines that can promote coordination or H-bonding at these sites. The reaction of 2,1,3-benzothiadiazole-4,5-diamine **9** with **1** resulted in the asymmetric **12** with high yields. The molecule **12** has a low solubility in most solvents. The diamine **10** was reacted with **1** in 1:1 water/ethanol v/v resulting in the dipyrido[3,2-*a*:2′,3′-*c*]phenazine-11-sulfonic acid **13**, that shows a increased solubility in water and in mixtures of water/ethanol and water/DMSO, an important feature for biochemistry studies (Scheme 2).

The ^1H NMR spectrum of **11** shows five peaks due to the C_{2v} symmetry (see Supplementary data, Fig. S1), and the assignment of the signals are in agreement with the literature, where the H_c proton is the most shifted to high fields while the H_b proton is less affected when compared to the other protons in dppz and phen systems.[25,26] On the other hand, the phenanthroline moiety of compound **12** is considerably affected by the thiadiazole conjugate group at the 10 and 11 positions, the H_c and H_c' are separated by 0.25 ppm (see Supplementary data, Fig. S2). The protons H_a/H_a' and H_b/H_b' are less affected by the geometry of the molecule and occur in the same peak, each signal in these cases referring to two protons. It can be noted that there are 18 peaks in the ^{13}C spectrum of **12**, which shows that the carbon atoms are more affected by molecular asymmetry than the hydrogen atoms. The ^1H NMR spectrum of compound **13** shows that it is less affected than compound **12**, having six peaks due to its molecular geometry (see Supplementary data, Fig. S3). The protons in the phenanthroline moieties are not separated in either case, and the ^{13}C NMR shows 16 peaks, the other two peaks are in the region of CF_3CO_2D. Also,

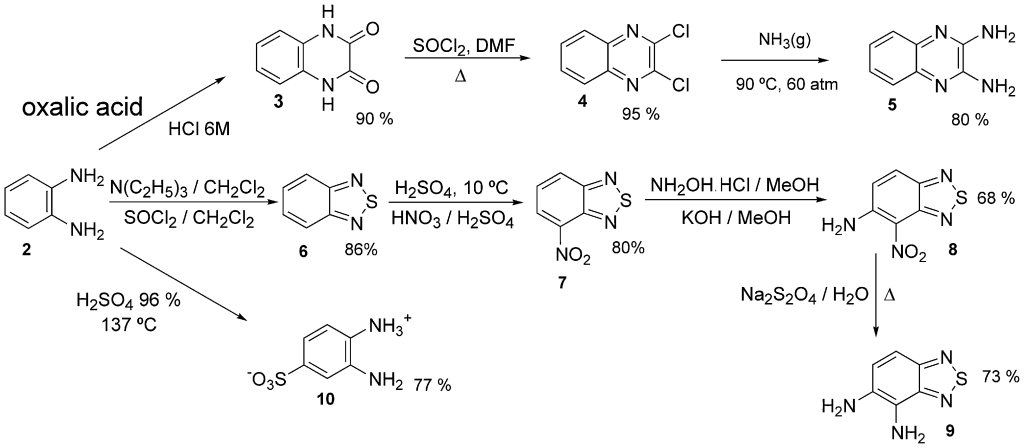

Scheme 1. Synthesis of diamines.

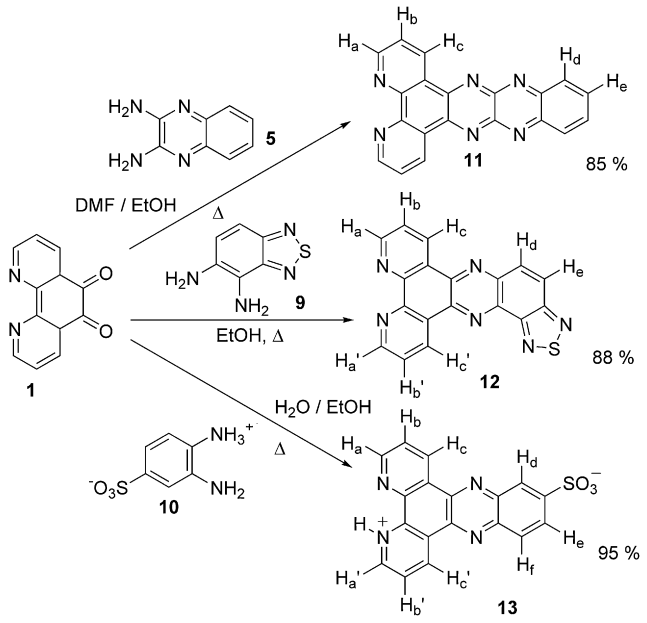

Scheme 2. Synthesis of new dppz ligands.

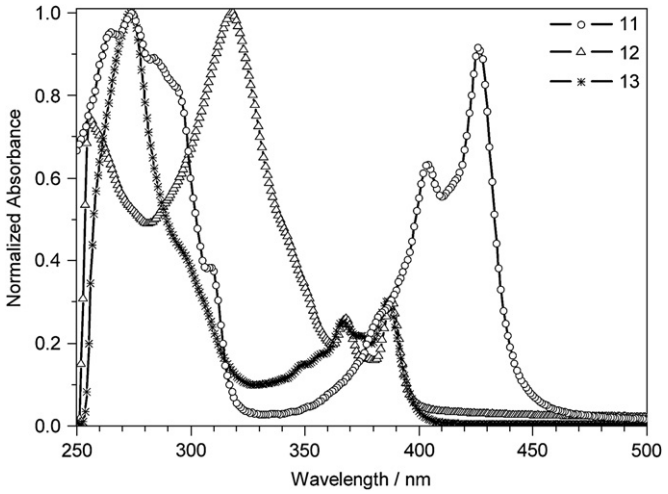

Figure 1. Absorption spectra of **11**–**13** in DMSO at 3×10^{-5} M.

compound **13** behaves in the same way as compound **12**, which confirms the influence of substituent groups on the carbon atoms in all parts of the extended conjugate π-system.

The electrochemical, spectroscopic, and DFT results are summarized in Table 1. The UV–visible spectrum of **11** in DMSO solution shows a different pattern when compared with the spectra of dpq and dppz (see Fig. 1), most probably due to the increase in number of pyrazine rings conjugated in the polycyclic system.[27] The spectrum shows two main peaks or regions, with three shoulders. The peaks in the region between 250–330 nm are not well defined and probably include the contribution of π–π* transitions of all parts of the ring and is also a characteristic of the π–π* transitions of the phenanthroline portion. The peak at 276 nm is tentatively assigned to the π–π* transition of the phenanthroline moiety. The strong absorption between 360–460 nm with two maxima at 409 and 432 nm is due to increased conjugation in the system and these maxima represent π–π* transitions. Compounds **12** and **13** exhibited the pattern of the dppz skeleton, the exception in **12** is the π–π* of the thiadiazole ring at 318 nm. The π–π* transitions of the phenanthroline moiety were observed at 256 and 260 nm, respectively, for **12** and **13**. In the literature, the other peaks are usually assigned to π–π* transitions of the pyrazine moiety. The electronic spectra of dpq,[28] dppz,[29,30] phenanthroline,[31] quinoxaline,[32] phenazine,[32] and tetraazanaphthacence[27] have been reported by many different groups. This information is important in the assignment of π–π* transitions relating to phenanthroline and pyrazine moieties, but a complete study is beyond the scope of this paper and an experimental and theoretical study on the excited states of these new compounds and their coordination compounds will be presented elsewhere.

Table 1
Summary of the results for the spectroscopic, electrochemical, and DFT calculations

Compound	Absorption spectra			Electrochemistry		pK_a	Results from DFT calculation at B3LYP/6-31+G(d,p)[a]									
	λ_{max}	log ε	Assignment	$E_{1/2}$, V	Assignment		HOMO	LUMO	Gap	$LUMO_{+1}$	$LUMO_{+2}$	χ	η	I	A	ω
11	269	4.69	π–π* phen	−0.422	π* taz	1.50	−6.75	−3.59	3.16	−2.00	−1.91	5.17	1.58	6.75	3.59	8.47
	276	4.71	π–π* phen	−0.787	π* taz	2.04	−6.78	−3.68	3.10	−2.06	−2.02	5.23	1.55	6.78	3.68	8.83
	286	4.68	π–π* phen	−1.029	π* taz	2.68										
	293	4.65	π–π* phen	−2.202	π* phen											
	310	4.38	π–π* taz	−2.393	π* phen											
	389	4.15	π–π* taz													
	409	4.48	π–π* taz													
	432	4.63	π–π* taz													
12	256	4.55	π–π* phen	−0.902	π* diaz	ND	−6.83	−2.87	3.97	−2.84	−1.89	4.85	1.98	6.83	2.87	5.93
	318	4.58	π–π* Thiadiazole	−1.174	π* diaz		−6.80	−2.87	3.93	−2.80	−1.97	4.84	1.96	6.80	2.87	5.95
	343	4.40	π–π* diaz	−1.568	π* diaz											
	351	4.27	π–π* diaz	−1.865	π* phen											
	367	4.16	π–π* diaz	−2.159	π* phen											
	377	3.97	π–π* diaz	−2.460	π* phen											
	387	4.26														
13	273	4.77	π–π* phen	−0.489	$-SO_3^-$	3.26	−5.18	−4.41	0.77	−3.74	−3.17	4.80	0.38	5.18	4.41	29.96
	295	4.41	π–π* phen	−0.879	$-SO_3^-$		−7.01	−3.20	3.81	−3.15	−2.41	5.11	1.91	7.01	3.20	6.84
	347	3.97	π–π* diaz	−1.192	π* diaz		−7.05	3.29	3.77	−2.31	−2.06	5.17	1.88	7.05	3.29	7.10
	355	4.02	π–π* diaz	−1.820	π* phen		−6.90	−3.12	3.78	−2.15	−1.99	5.01	1.89	6.90	3.12	6.63
	366	4.17	π–π* diaz	−2.022	π* phen		−2.99	−0.44	2.56	0.06	0.25	1.72	1.28	2.99	0.44	1.15
	375	4.12	π–π* diaz	−2.181	π* phen		−6.60	−2.76	3.84	−1.84	−1.82	4.68	1.92	6.60	2.76	5.71
	386	4.27	π–π* diaz	−2.338	π* phen											
				−2.404	π* phen											

ND—not determined; taz—tetraza; diaz—diazine.

[a] The theoretical results are shown in the following order, first line gaseous phase and below the DMSO phase. In the case of compound **13** the results are expressed as the two first lines zwitterionic form, the next two lines the neutral form, and the last lines the anionic form.

The easy reduction of dipyridophenazines is due to the lower energy π^* orbital of the phenazine moiety.[29] Thus, the π-accepting site in dipyridophenazine is located on the phenazine portion of the molecule. DFT calculations are known to provide good geometries, frequencies, and ground-state energies. We used the B3LYP/6-31+G(d,p) method to correlate the electronic structure of compounds **11**–**13** with the electrochemical properties.

For this correlation we used the conceptual DFT,[33–35] whereby it is possible to calculate the theoretical values of electronegativity (χ), hardness (η), ionization energy (I), electronic affinity (A), and electrophilicity index (ω), among other properties. All these properties are calculated from the energies of frontier orbitals and the mathematical formalism can be found in the Refs. 33–35. Table 1 shows the values of HOMO, LUMO, $LUMO_{+1}$, $LUMO_{+2}$, gap, ionization energy, electronic affinity, and electrophilicity index in gaseous and liquid phase (DMSO) calculated by the PCM method. In the case of compound **13** we decided to explore the three different forms of protonation: (a) the zwitterionic form with the nitrogen from the protonated phenanthroline moiety; (b) the anionic form and (c) the neutral form with the protonation at the sulfonic group. The zwitterionic form was found to be more stable than the neutral form by 10.33 kcal mol^{-1} in aqueous phase and 9.86 kcal mol^{-1} in DMSO phase. An inverse situation is found in the gaseous phase where the neutral form is 23.83 kcal mol^{-1} more stable than the zwitterionic form. This situation shows the importance of the inclusion of solvent effects in order to obtain correct predictions of molecules, which can present different possibilities of protonation.

Comparison of the first reduction process of **11**–**13** with dpq and dppz shows a shift in the reduction process to positive values in **11** due to the extended conjugate system, which facilitates the reduction process. The analysis of the molecular orbital is important to determine the electrochemically active orbital, since the first LUMO is called the electrochemical orbital.[25,30] For molecule **11**, the first LUMO is tetraza based, and thus the first reduction process will probably occur at this site. But the other LUMOs have close energy values allowing, also, the population of these electronic states. This is currently being investigated by ab initio calculations and experimental techniques and the results will be presented in the future.

The square wave voltammogram of **11** shows five successive reduction processes (see Fig. 2). The first at −0.422 V is reversible while the others at −0.787, −1.029, −2.202, and −2.393 V are quasi-reversible. The three empty orbitals of lower energy are very different, the LUMO shows more contribution from tetraza moiety, while the $LUMO_{+1}$ is completely extended throughout the system and the $LUMO_{+2}$ has a contribution only from the phenanthroline moiety. The LUMO and $LUMO_{+1}$ probably participate in the process between 0.4–1.0 V while the $LUMO_{2+}$ is in agreement with the high reduction potentials of the phenanthroline moiety (see Supplementary data, Fig. S5). It is important to note that $LUMO_{+1}$ and $LUMO_{+2}$ orbitals probably participate in the charge transfer from metal to ligand in the complex, because the symmetry is appropriate and the nitrogens of phenanthroline have a significant participation in these molecular orbitals. Ligand **12** has six reduction processes at −0.902, −1.174 V (reversible and phenazine based), −1.568, −1.865, −2.159, and −2.460 V (quasi-reversible) assigned to phenanthroline site reduction. The plot of the molecular orbital of **12** in particularly the LUMOs showed a similar behavior to **11** (see Supplementary data, Fig. S6), i.e., the LUMO and $LUMO_{+1}$ are phenazine centered and $LUMO_{+2}$ is phenanthroline based. The difference is the delocalization caused by the asymmetry of the molecular shape. Regarding the electrochemistry of **13** there are two main reduction peaks at −1.192 and −2.404 V, the first one assigned to the phenazine part and the second to the phenanthroline moiety, however, the molecule has another six peaks from the reduction reactions of the sulfonic group at −0.489, −0.879, −1.820, −2.022, −2.181, and −2.338 V. However, the square wave voltammetry starting at negative potentials shows two oxidation peaks at −0.192 and 0.113 V, due to the re-oxidation of sulfonic groups reduced at low potentials.

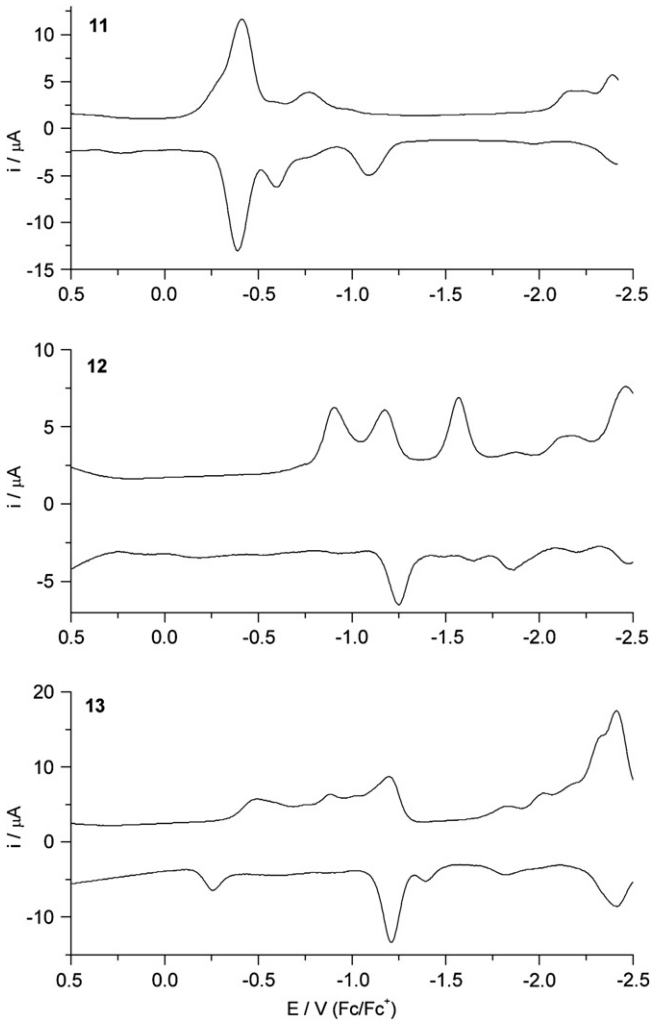

Figure 2. Square wave voltammograms of **11**–**13** at 10^{-3} M in DMSO.

Of the theoretically calculated parameters the best correlation of the electrochemical results was found between electronic affinity and the electrophilicity index in the DMSO phase. These parameters expressed the tendencies of a certain molecule to undergo reduction. The usefulness of electrophilicity index has also been reported in other contexts.[36,37] The comparison shows that molecule **11** possesses a high electron acceptor characteristic because of the high values of A and ω. Molecule **13** shows a tendency to undergo reduction of the sulfonic group. The best correlation was found in DMSO due to the instability of the zwitterionic form in gaseous phases. The molecular orbitals were more affected by solvent inclusion in **13** than in the cases of **11** where they do not change forms, and **12**, where they showed few modifications in the LUMO and $LUMO_{+1}$. The changes caused by solvent inclusion are more evident in the ionic forms of **13** where there is high charge concentration in specific parts.

The pK_a's of **11** and **13** were determined by potentiometric titration in a 70:30 ethanol/water system. The values found for the hydrolysis of the phenanthroline moiety were 2.68 and 3.26, respectively, for **11** and **13**. These pK_a's values are in agreement with the phenanthroline protonation as described in the literature.[38] Compound **13** showed a maximum solubility at pH=3.40, indicating the best pH to work with it. Compound **11** shows two further pK_a's of 1.50 and 2.04, which are assigned to the tetraza

portion. The pK_a of **12** was not determined because of the low solubility of this compound.

Compounds **10**–**13** were characterized by ^{1}H and ^{13}C NMR, infrared, mass spectroscopy, and elemental analysis. Compounds **1** and **3**–**9** were prepared according to the literature, giving spectral data consistent with that reported. Confirmatory characterization is provided in Supplementary data.

Compounds **11**–**13** are being tested as DNA intercalating agents, such as ruthenium complexes ($[Ru(phen)_2L]^{2+}$) and iron(II) tris-complexes, and the results will be presented in future papers.

2. Experimental

2.1. General

All reagents and solvents for the synthesis and analysis were of analytical and/or spectroscopic grade from Sigma or Aldrich and used without further purification. Infrared spectra were acquired on a Perkin Elmer FTIR 2000. NMR analysis was performed on a Varian 400 MHz spectrometer. Elemental analysis for compounds **10**–**13** was carried out using a Carlo Erba Analyzer Model E-1110. The UV–visible spectra were obtained using a Perkin Elmer Lambda 19 instrument. Low-resolution mass spectra were obtained for compounds **1** and **3**–**12** on a Shimadzu CGMS-QP5050A instrument using the direct injection mode. The samples were placed in a sample vial fixed onto the probe. The probe temperatures were programmed as follows: 5 °C min^{-1} up to 100 °C and held for 5 min, increasing from 100 to 300 °C at 20 °C min^{-1}, and held for 5 min. The quadrupole mass spectrometer was operated in the electron impact (EI) mode (ionization energy 70 eV) scanning from m/z 20 to 400 in 0.5 s. The mass spectra for compound **13** was obtained by ESI-MS. The ESI-Q-Tof mass spectrometry (MS) analyses were carried out using a Q-Tof ultima API spectrometer (Waters/Micromass) equipped with an elecrospray ionization source operated in the negative mode (ESI(−)-MS). Typical MS conditions were: source temperature of 100 °C, dessolvation temperature of 100 °C, capillary voltage of 3.5 kV and cone voltage of 35 V. Mass spectrometer calibrations were made by using formic acid. Compound **13** was diluted in water, acetonitrile, and formic acid (50:49.9:0.1, v/v/v). The sample was injected using a syringe pump at a flow rate of 10 μL min^{-1}. Mass spectra were acquired along m/z 100–1500 range. Data were analyzed by MassLynx® 4.0 software. The electrochemical experiments were carried with deaerated 3×10^{-4} mol L^{-1} solutions of compounds **11**–**13**, all in DMSO. The experiments were performed using Pt working and auxiliary electrodes, an Ag/AgCl reference electrode, and Bu_4NPF_6 at a concentration of 0.1 mol L^{-1} as the supporting electrolyte. The ferrocene–ferrocenium (Fc/Fc^+) couple served as the internal reference,[39] and all potentials were referenced to normal hydrogen electrode (0.400 V vs NHE). The instrument used was a BASI Epsilon Model EC Epsilon. The square wave voltammetry was performed at frequency of 25 Hz and amplitude of 10 Hz. Cyclic voltammetry used scan rates of 50, 100, 200, 300 mV s^{-1}. The pKa's of **11** and **13** were determined by potentiometric titration in an ethanol/water mixture (as described in literature[40]), with the aid of the BEST7 program.[41] All calculations reported here were performed by the Gaussian 03 code.[42] B3LYP exchange correlation potential,[43] in connection with the 6-31+G(d,p) basis set, were used to obtain equilibrium geometries of the new molecules. Harmonic vibration frequencies were computed to characterize them as minima energy point. To study the solution behavior of the different species, the polarized continuum (overlapping spheres) model[44] was used, to simulate the water and DMSO solvents. PCM calculation used radii UAKS and all standard specifications of Gaussian package, the exception was the electrostatic scaling factor of 1.35 to DMSO.

2.2. Synthesis

*2.2.1. 3,4-Diaminobenzenesulfonic acid (**10**)*

Compound **2** (20 g, 184.94 mmol) was added to 90 mL of sulfuric acid 96% at −30 °C under stirring for 1 h, followed by stirring until room temperature. The green solution was then kept at 137 °C for 1 day. The reaction mixture was cooled and cold water was added to afford a white precipitate, which was filtered off and recrystallized in water to afford white crystals. Yield 77%. Anal. Calcd for $C_6H_8N_2O_3S\cdot2H_2O$: C, 32.14; H, 5.39; N, 12.49; S, 14.30. Found: C, 31.98; H, 5.23; N, 12.12; S, 14.28. MS (EI, 70 eV) m/z 188.05 [M$^+$], calcd 188.03. ^{1}H NMR (ppm, 400 MHz, D_2O) δ: 6.82 (d, J_3=8.4 Hz, 1H), 7.17 (dd, J_3=8.4 Hz, J_4=1.8 Hz, 1H), 7.36 (d, J_4=1.8 Hz, 1H), 8.1 (br s, 4H). ^{13}C NMR (ppm, 100.8 MHz, D_2O) δ: 117.1, 118.1, 119.3, 122.5, 133.3, 135.5. IR (KBr, cm^{-1}): 3058, 1682, 1568, 1457, 1411, 1312, 1289, 1202, 1114, 1007, 921, 810, 736.

*2.2.2. Dipyrido[3,2-f:2′,3′-h]quinoxalino[2,3-b]quinoxaline (dpq-QX) or quinoxalino[2′,3′:5,6]pyrazino[2,3-f][1,10]-phenanthroline (**11**)*

Compound **1** (1 g, 4.76 mmol) was dissolved in ethanol under nitrogen and 0.78 g (4.87 mmol) of **5** dissolved in DMF was added to this solution and the reaction mixture was then refluxed for 8 h. The orange solid formed was filtered off and washed with cold water, ethanol, and acetone. The product was recrystallized in chloroform to afford an orange material. Yield 85%. Anal. Calcd for $C_{20}H_{10}H_6\cdot0.8H_2O$: C, 68.87; H, 3.36; N, 24.10. Found: C, 68.58; H, 3.15; N. 24.15. MS (EI, 70 eV) m/z 334.15 [M$^+$], calcd 334.10. ^{1}H NMR (ppm, 400 MHz, $CDCl_3$) δ: 7.88 (dd, J_3=8.1, 4.4 Hz, 2H, H_b), 8.07 (dd, J_3=7.0 Hz, J_4=3.3 Hz, 2H, H_e), 8.52 (dd, J_3=7.0 Hz, J_4=3.3 Hz, 2H, H_d), 9.35 (dd, J_3=4.4 Hz, J_4=1.5 Hz, 2H, H_a), 9.83 (dd, J_3=8.1 Hz, J_4=1.5 Hz, 2H, H_c). ^{13}C NMR (ppm, 100.8 MHz, $CDCl_3$) δ: 109.7, 124.9, 126.9, 130.2, 133.1, 135.4, 143.7, 146.6, 146.9, 154.2. UV–vis (DMSO, nm (log ε)): 269 (4.69), 276 (4.71), 286 (4.68), 293 (4.65), 310(4.38), 389 (4.15), 410 (4.48), 432 (4.63). IR (KBr, cm^{-1}): 3079, 1582, 1493, 1412, 1385, 1203, 1080, 894, 753, 740, 503.

*2.2.3. Dipyrido[3,2-a:2′,3′-c]phenazine-10,11-(2,1,3-thiadiazole) (dppz–BTDZ) (**12**)*

Compound **1** (1 g, 4.76 mmol) was dissolved in ethanol under nitrogen and 0.80 g (4.81 mmol) **9** was added to this solution and the reaction mixture was stirred for 15 min at room temperature and then refluxed for further 2 h. The solid formed was filtered off and washed with water, cold ethanol, hexane, and acetone. The product was recrystallized in dichloromethane to afford a pink material. Yield 88%. Anal. Calcd for $C_{18}H_{10}N_6S\cdot0.5H_2O$: C, 61.88; H, 2.60; N, 24.05; S, 9.18. Found: C, 61.51; H, 2.45; N, 23.91; S, 8.96. MS (EI, 70 eV) m/z 340.25 [M$^+$], calcd 340.05. ^{1}H NMR (ppm, 400 MHz, CF_3CO_2D) δ: 8.56 (dd, J_3=8.4, 5.1 Hz, 2H, H_b/H_b'), 8.66 (d, J_3=8.8 Hz, 1H, H_e), 8.72 (d, J_3=8.8 Hz, 1H, H_d), 9.54 (dd, J_3=5.1 Hz, J_4=1.5 Hz, 2H, H_a/H_a'), 10.43 (dd, J_3=8.4 Hz, J_4=1.5 Hz, 1H, H_c), 10.67 (dd, J_3=8.4 Hz, J_4=1.5 Hz, 1H, H_c'). ^{13}C NMR (ppm, 100.8 MHz, trifluoroacetic-d_1) δ: 126.1, 127.6, 127.6, 129.9, 130.1, 132.8, 138.2, 138.4, 139.1, 139.2, 140.1, 140.6, 141.1, 146.7, 148.3, 148.6, 152.1, 156.3; UV–vis (DMSO, nm (log ε)): 256 (4.55), 318 (4.58), 343 (4.40), 351 (4.27), 367 (4.16), 377 (3.97), 387 (4.26). IR (KBr, cm^{-1}): 3024, 1573, 1492, 1422, 1375, 1364, 1129, 1084, 1078, 836, 817, 741, 497.

*2.2.4. Dipyrido[3,2-a:2′,3′-c]phenazine-11-sulphonic acid (dppz–SO_3) (**13**)*

A mixture of 1 g (4.76 mmol) of 1,10-phenanthroline-5,6-dione and 1.08 g (4.83 mmol) of **10** in 20 mL of water/ethanol 1:1 v/v was refluxed for 4 h. Upon cooling, the white-yellow precipitate was collected by filtration and washed with cold water, methanol, and acetone. Yield 95%. Anal. Calcd for $C_{18}N_4H_9SO_3H$: C, 59.66; H, 2.78;

N, 15.46; S, 8.85. Found: C, 59.35; H, 2.76; N, 15.28; S, 8.66. ESI-MS (−) *m*/*z* 361.037 [M$^-$], calcd 361.039. ^{1}H NMR (ppm, 400 MHz, CF_3CO_2D) δ: 9.60 (dd, J_3=8.1, 5.1 Hz, 2H, H_b/H_b'), 9.70 (d, J_3=9.0 Hz, 1H, H_f), 9.77 (d, J_3=9.0 Hz, 1H, H_e), 10.19 (s, 1H, H_d), 10.55 (dd, J_3=5.1 Hz, J_4=1.5 Hz, 2H, H_a/H_a'), 11.40 (dd, J_3=8.1 Hz, J_4=1.5 Hz, 2H, H_c/H_c'). ^{13}C NMR (ppm, 100.8 MHz, trifluoroacetic-d_1) δ: 128.8, 129.1, 130.4, 131.0, 131.0, 132.0, 140.2, 140.4, 140.9, 141.7, 141.9, 143.0, 144.9, 146.0, 149.2, 149.6. UV–vis (DMSO, nm (log ε)): 273 (4.76), 295 (4.41), 347 (3.97), 355 (4.02), 366 (4.17), 375 (4.11), 386 (4.27). IR (KBr, cm^{-1}): 3082, 2757, 1613, 1446, 1414, 1354, 1257, 1247, 1027, 726, 674.

Acknowledgements

The authors are grateful to CNPq for the financial grant (process 478999/2003-8) and the fellowship research, to UFSC, the technical staff of Central de Análises DQ/UFSC, Ângelo Ruzza by NMR spectra, to Professor Faruk Nome for the use of the mass spectroscopy equipment and to Anderson Bastos Pires by the chemical equilibrium studies.

Supplementary data

The confirmatory analysis for compounds **1**, **3**–**9**. ^{1}H NMR spectra of **11**–**13** (Figs. S1–S3), the cyclic voltammograms (Figs. S4), molecular orbital and electrostatic potential surfaces plots are provided as supplementary data (Figs. S5–S9). Supplementary data associated with this article can be found in the online version, at doi:10.1016/j.tet.2008.02.097.

References and notes

1. Yam, V. W. W.; Ko, C. C.; Zhu, N. *J. Am. Chem. Soc.* **2004**, *126*, 12734–12735.
2. Kopelman, R. A.; Snyder, S. M.; Frank, N. L. *J. Am. Chem. Soc.* **2003**, *125*, 13684–13685.
3. Erkkila, K. E.; Odom, D. T.; Barton, J. K. *Chem. Rev.* **1999**, *99*, 2777–2796.
4. Thomas, A. M.; Nethaji, M.; Chakravarty, A. R. *J. Inorg. Biochem.* **2004**, *98*, 1087–1094.
5. Roy, M.; Saha, S.; Patra, A. K.; Nethaji, M.; Chakravarty, A. R. *Inorg. Chem.* **2007**, *46*, 4368–4370.
6. Roelfs, G.; Feringa, B. L. *Angew. Chem., Int. Ed.* **2005**, *44*, 3230–3232.
7. Kwan, P. H.; Maclachlan, M. J.; Swager, T. M. *J. Am. Chem. Soc.* **2004**, *126*, 8638–8639.
8. Pabst, G. R.; Pfüller, O. C.; Sauer, J. *Tetrahedron Lett.* **1998**, *39*, 8825–8828.
9. Fees, J.; Kaim, W.; Moscherosch, M.; Matheis, W.; Klíma, J.; Krejeík, M.; Zális, S. *Inorg. Chem.* **1993**, *32*, 166–174.
10. Dickeson, J. E.; Summers, L. A. *Aust. J. Chem.* **1970**, *23*, 1023–1027.
11. Amouyal, E.; Homsi, A.; Chambron, J.-C.; Sauvage, J.-P. *J. Chem. Soc., Dalton Trans.* **1990**, 1841–1845.
12. Neves, A.; Lanznaster, M.; Bortoluzzi, A. J.; Peralta, R. A.; Casellato, A.; Castellano, E. E.; Herrald, P.; Riley, M. J.; Schenk, G. *J. Am. Chem. Soc.* **2007**, *129*, 7486–7487.
13. Peralta, R. A.; Neves, A.; Bortoluzzi, A. J.; dos Anjos, A.; Xavier, F. R.; Szpoganicz, B.; Terenzi, H.; de Oliveira, M. C. B.; Castellano, E.; Friedermann, G. R.; Mangrich, A. S.; Novak, M. A. *J. Inorg. Biochem.* **2006**, *100*, 992–1004.
14. Cotton, F. A.; Chun, Z. L.; Murillo, C. A.; Villagrán, D. *Inorg. Chem.* **2006**, *45*, 767–778.
15. Tadokoro, M.; Yasuzuka, S.; Nakamura, M.; Shinoda, T.; Tatenuma, T.; Mitsumi, M.; Ozawa, Y.; Toriumi, K.; Yoshino, H.; Shiomi, D.; Sato, K.; Takui, T.; Mori, T.; Murata, K. *Angew. Chem., Int. Ed.* **2006**, *45*, 5144–5147.
16. Hino, S.; Kato, M.; Nakamura, M.; Tadokoro, M. *Mol. Cryst. Liq. Cryst.* **2006**, *455*, 205–209.
17. Komin, A. P.; Carmack, M. *J. Heterocycl. Chem.* **1976**, *13*, 13–22.
18. Neto, B. A. D.; Lopes, A. S. A.; Ebeling, G.; Gonçalves, R. S.; Costa, V. E. U.; Quina, F. H.; Dupont, J. *Tetrahedron* **2005**, *61*, 10975–10982.
19. Komin, A. P.; Carmack, M. *J. Heterocycl. Chem.* **1975**, *12*, 829–833.
20. Cillo, C. M.; Lash, T. D. *J. Heterocycl. Chem.* **2004**, *41*, 955–962.
21. Rauchschwalbe, G.; Emde, H.; Kissener, W. U.S. Patent 6,787,666, 2004.
22. Rauchschwalbe, G.; Emde, H.; Kissener, W. EP Patent 1 400 507, 2003.
23. Nakata, K.; Shimomura, N.; Shiina, N.; Izumi, M.; Ichikawa, K.; Shiro, M. *J. Inorg. Biochem.* **2002**, *89*, 255–266.
24. Paw, W.; Eisenberg, R. *Inorg. Chem.* **1997**, 2287–2293.
25. Arancibia, A.; Concepción, J.; Daire, N.; Leiva, G.; Leiva, A. M.; Loeb, B.; Del Río, R.; Díaz, R.; Francois, A.; Saldivia, M. *J. Coord. Chem.* **2001**, *54*, 323–336.
26. Ivanov, M. A.; Puzyk, M. V.; Balashev, K. P. *Russ. J. Gen. Chem.* **2006**, *76*, 881–886.
27. Kuhn, R.; Skrabal, P.; Fischer, P. H. H. *Tetrahedron* **1968**, 1843–1849.
28. Van Der Tol, E. B.; Van Ramesdonk, H. J.; Verhoeven, J. W.; Steemers, F. J.; Kerver, E. G.; Verboom, W.; Reinhoudt, D. N. *Chem.—Eur. J.* **1998**, *4*, 2315–2323.
29. Yamada, M.; Tanaka, Y.; Yoshimoto, Y.; Kuroda, S.; Shimao, I. *Bull. Chem. Soc. Jpn.* **1992**, *65*, 1006–1011.
30. Juliarema, M. P.; Lezna, R. O.; Feliz, M. R.; Ruiz, G. T.; Thomas, S.; Ferraudi, G.; Carmichael, I. *J. Org. Chem.* **2006**, *71*, 2870–2873.
31. Yamada, M.; Kimura, M.; Nishizawa, M.; Kuroda, S.; Shimao, I. *Bull. Chem. Soc. Jpn.* **1991**, *64*, 1821–1827.
32. Badger, G. M.; Walker, I. S. *J. Chem. Soc.* **1956**, 122–126.
33. Proft, F. D.; Geerlings, P. *Chem. Rev.* **2001**, *101*, 1451–1464.
34. Geerlings, P.; Proft, F. D.; Langenaeker, W. *Chem. Rev.* **2003**, *103*, 1793–1873.
35. Chattaraj, P. K.; Sarkar, U.; Roy, D. R. *Chem. Rev.* **2006**, *106*, 2065–2091.
36. Parthasarathi, R.; Subramanian, V.; Roy, D. R.; Chattaraj, P. K. *Bioorg. Med. Chem.* **2004**, *12*, 5533–5543.
37. Roy, D. R.; Parthasarathi, R.; Maiti, B.; Subramanian, V.; Chattaraj, P. K. *Bioorg. Med. Chem.* **2005**, *13*, 3405–3412.
38. Martell, A. E.; Smith, R. M.; Motekaitis, R. J. *In Critically Selected Stability Constants of Metal Complex, NIST–Database 46*; NIST: Gaithersburg, MD, 2004.
39. Gagné, R. R.; Koval, C. A.; Lisensky, G. C. *Inorg. Chem.* **1980**, *19*, 2854–2855.
40. Schwingel, E. W.; Arend, K.; Zarling, J.; Neves, A.; Szpoganicz, B. *J. Braz. Chem. Soc.* **1996**, *7*, 31–37.
41. Martell, A. E.; Motekaitis, R. J. *The Determination and Use of Stability Constants*; VCH: New York, NY, 1990.
42. Frisch, M. J.; Trucks, G. W.; Schlegel, H. B.; Scuseria, G. E.; Robb, M. A.; Cheeseman, J. R.; Montgomery, J. A.; Vreven, T., Jr.; Kudin, K. N.; Burant, J. C.; Millam, J. M.; Iyengar, S. S.; Tomasi, J.; Barone, V.; Mennucci, B.; Cossi, M.; Scalmani, G.; Rega, N.; Petersson, G. A.; Nakatsuji, H.; Hada, M.; Ehara, M.; Toyota, K.; Fukuda, R.; Hasegawa, J.; Ishida, M.; Nakajima, T.; Honda, Y.; Kitao, O.; Nakai, H.; Klene, M.; Li, X.; Knox, J. E.; Hratchian, H. P.; Cross, J. B.; Adamo, C.; Jaramillo, J.; Gomperts, R.; Stratmann, R. E.; Yazyev, O.; Austin, A. J.; Cammi, R.; Pomelli, C.; Ochterski, J. W.; Ayala, P. Y.; Morokuma, K.; Voth, G. A.; Salvador, P.; Dannenberg, J. J.; Zakrzewski, V. G.; Dapprich, S.; Daniels, A. D.; Strain, M. C.; Farkas, O.; Malick, D. K.; Rabuck, A. D.; Raghavachari, K.; Foresman, J. B.; Ortiz, J. V.; Cui, Q.; Baboul, A. G.; Clifford, S.; Cioslowski, J.; Stefanov, B. B.; Liu, G.; Liashenko, A.; Piskorz, P.; Komaromi, I.; Martin, R. L.; Fox, D. J.; Keith, T.; Al-Laham, M. A.; Peng, C. Y.; Nanayakkara, A.; Challacombe, M.; Gill, P. M. W.; Johnson, B.; Chen, W.; Wong, M. W.; Gonzalez, C.; Pople, J. A. *Gaussian 03, Revision A.1*; Gaussian: Pittsburgh, PA, 2003.
43. Becke, A. D. *J. Chem. Phys.* **1993**, *98*, 5648–5652.
44. Miertus, S.; Scrocco, E.; Tomasi, J. *Chem. Phys.* **1981**, *55*, 117–129.